ChemComm

FEATURE ARTICLE

View Article Online
View Journal | View Issue

Check for updates

Cite this: *Chem. Commun.*, 2025, **61**, 5410

Zero-discharge, self-sustained 3D-printed microbial electrolysis cell for biohydrogen production: a review

Mandar S. Bhagat, *[a] Chirag Mevada, *[b] Jaini Shah,[a] M. Abdul Rasheed[a] and Matti Mäntysalo[b]

Microbial fuel cell (MFC) and microbial electrolysis cell (MEC) technologies have been used recently in bench-scale bioenergy (electricity) generation, biohydrogen (H_2) production, biosensing, and wastewater treatment. There are still a lot of obstacles to overcome in terms of commercialization and industrial settling. These difficulties include lengthy start-up times, intricate reactor designs for managing large reaction volumes, and expensive and time-consuming large-scale system fabrication procedures. Interestingly, combining three-dimensional (3D) printing with MFC and MEC technology appears to be a workable and promising way to get past these obstacles. Moreover, a rapid start-up with no delays in the current generation using MFC and MEC is possible with 3D printed bio-anodes. Furthermore, H_2 can be generated from wastewater by powering a stacked MFC and MEC-coupled with electrochemical capacitor (ECC) system using 3D printing technology. To the best of the author's knowledge, this review paper is the first to explicitly highlight the use of 3D printing in creating a stacked MFC–ECC–MEC system in conjunction with a photobioreactor (PBR) to produce significant quantities of H_2 and carbon dioxide (CO_2) can be utilized for algae production. A notable feature of 3D printing technology is its reliable production capabilities, enabling MFC–ECC–MEC–PBR systems to be expanded by setting up numerous stacks of MFC–ECC–MEC–PBR units devoid of material waste and human error. The present review attempts to provide an update on the current status of the 3D printing application, that is meant to propel the MFC–ECC–MEC–PBR system forward.

Received 7th January 2025,
Accepted 6th March 2025

DOI: 10.1039/d5cc00103j

rsc.li/chemcomm

Open Access Article. Published on 29 1403. Downloaded on 17/02/1405 01:20:45 ..
This article is licensed under a Creative Commons Attribution-NonCommercial 3.0 Unported Licence.

1. Introduction

Meeting the world's energy needs in the face of an ever-growing population has emerged as humanity's greatest challenge. As the population has increased over time, so need for energy, growing exponentially.[1] Nevertheless, we rely primarily on fossil fuels to meet our energy needs. We use coal, oil, and other fossil fuels to meet our needs, that eventually leads to the release of pollutants into the environment and the need for additional remediation. Presently, the majority of international and national organizations have implemented policies designed to increase the total amount of "green" energy produced while reducing emissions of pollutants.[2] Biogas or bio-hydrogen (CH_4 or H_2) is gaining more attention globally, as an alternative clean energy source that may help reduce the use of fossil fuels and greenhouse gas (GHG) emissions.[3] Compared to hydrocarbon fuels, H_2 has 2.75 times more energy content (122 kJ g^{-1}).[4] It is nontoxic, colourless, tasteless, odourless, light, and environmental friendly. Water is the only by-product of combustion when it is used as fuel. Biological processes such as microbial electrolysis cell (MEC), which operate at room temperature and pressure with little energy consumption (approx. practical voltage up to 1 V), are a viable and clean way to produce H_2.[5] The use of MEC, to treat wastewater, make chemicals or biofuels, and generate electricity with minimal energy input has gained increased attention lately as potentially green approaches.[6,7]

In MEC, protons and electrons are produced by bacteria oxidizing organic matter in a microbial fuel cell (MFC).[8] Protons move from the electrolyte toward the cathode by diffusing. Current is produced as the electrons move through a circuit to reach the cathode. A species, like oxygen, combines with the protons and electrons at the cathode to create a reduced compound, like water. By removing oxygen at the cathode and introducing a modest voltage (up to 1 V) to the circuit, H_2 is produced at the cathode of a MEC.[9] MEC can break down a wide range of complex substrates, including end

[a] *Department of Environment Management, Gujarat Energy Research and Management Institute, Gandhinagar, Gujarat, India 382 007. E-mail: mandar.b@germi.res.in*
[b] *Faculty of Information Technology and Communication Sciences, Tampere University, Tampere, Finland. E-mail: chirag.mevada@tuni.fi*

 This journal is © The Royal Society of Chemistry 2025

Open Access Article. Published on 29 1403. Downloaded on 17/02/1405 01:20:45 ..
This article is licensed under a Creative Commons Attribution-NonCommercial 3.0 Unported Licence.

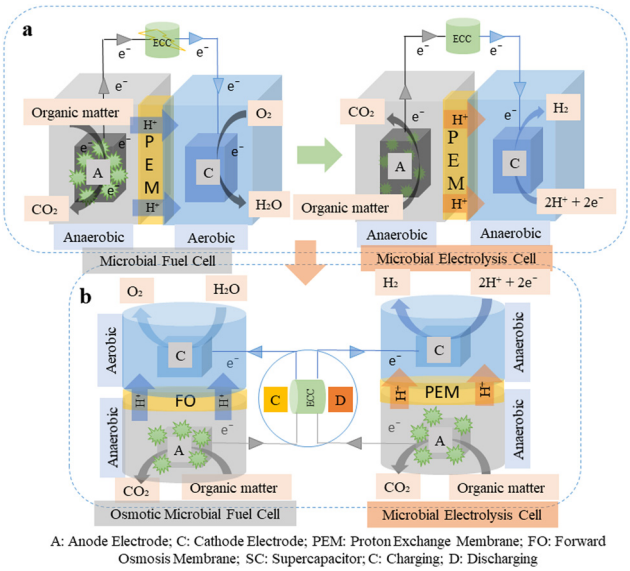

Fig. 1 Schematic of the (a) basic difference between MFC and MEC coupled with ECC and (b) OMFC and MEC system coupled with ECC (charging and discharging).

products from fermentation, pig dung, and household and commercial wastewater. The performance of these substrates is less in MEC than that of simple substrates such as cellulose, acetate, and glucose due to the partially degraded substrates.[5,6,9,10] Compared to alternative technologies like dark fermentation and photosynthesis, MEC are intriguing for producing H_2 because (1) they require a significantly lower energy input than water electrolysis, that produces H_2; and (2) they have a higher H_2 yield.[11] The schematic of the basic difference between MFC and MEC is shown in Fig. 1(a). On the contrary, the osmotic microbial fuel cell (OMFC) process that combines the benefits of both forward osmosis (FO) (transport of water molecules across a membrane from low to high osmotic pressure) and MFC to improve electricity performance. OMFC technology has drawn increasing attention owing to the growing demand for clean water and bioenergy sources. OMFC and MFC are novel approaches that combine electrochemistry and microbiological metabolism for a range of high-value applications.[12,13]

Electrochemical capacitors (ECCs) have attracted much attention lately as an incredibly affordable energy storage technology.[14,15] They offer advantages like rapid charging, more power output, and longer lifespans by using fast oxidation–reduction and ion adsorption processes.[2] The viability of combining ECC and MEC has recently been the subject of increasing research publications. Previously, it was proposed to use MFC to directly power MEC; however, the performance of the systems was limited by the low voltages produced when the two systems were directly connected.[16,17] In an MFC–ECC–MEC circuit, adding ECC improved system performance in terms of energy recovery, MEC yield, and H_2 production rates when the capacitance was adjusted to better match the charge generated by the MFCs. The ideal capacitance per MFC for the air-cathode, single chamber (SC) MFCs utilized here was 0.01 F. The capacitor circuit was added to the MFC–ECC–MEC system, increasing energy recoveries by 77%, MEC yields by 60%, and H_2 production rates by 38%.[17] A stacked MFCs used in parallel, or series allowed for quick charging of the ECC and efficient powering of the MEC.[18,19] On the contrary, microalgae in photobioreactors (PBR), could just as easily convert CO_2 (generated during microbial electrolysis in an anode chamber) into oxygen (O_2).[20] Carbon capture and wastewater treatment are currently possible with photobioreactor and MFC technologies.[21,22] The MFC–ECC–MEC–PBR system combines zero emission (converting CO_2 to O_2) and self-sustained technology, eliminating the need for additional power sources to operate the system. ECC can be charged by MFC or OMFC and discharged by the MEC system to produce H_2 through electrolysis, as shown in Fig. 1(b).

The field of MFC or MEC could undergo a revolutionary shift due to the potential for flexible and intricate design of electrochemically active materials, made possible by additive manufacturing, also referred to as 3-dimensional (3D) printing.[23–25] This technology has been a major driver of innovation in industrial manufacturing. Recent successful applications of the technology include enhanced electrochemical CO_2 reduction and the quick development and testing of customized electrode and reactor prototypes.[26,27] Apart from producing reactor parts, 3D printing holds great potential for creating next-generation electrodes since it allows for the production of materials with a large surface area and the ability to structure them at the nanoscale level through post-processing techniques.[26,28,29] It is possible to realize complex custom designs, such as the addition of flow channels to provide a high surface area per volume and the addition of a metallic core to provide high conductivity over large electrodes. Printing metal ink is one way to create conductive metal substrates. Furthermore, there are plans to 3D print metallic materials directly *via* electrochemical reduction of metal ions from solutions onto conductive substrates.[30,31]

The most recent Scopus data shows that, to date, ~2 and ~1216 research or review articles with the keywords 3D printed MEC and MEC for H_2 recovery, respectively, have been published.[32] These articles cover a range of MEC characteristics and operating conditions. In a recent study, the spiral computer-aided design (CAD) model is created with four counter-clockwise revolutions and a 0.5 cm pitch.[33] Selective laser sintering (SLS) 3D printing techniques are used to produce spiral electrodes with controlled porosity as well as interdigitated electrodes in desired electrode forms. As standard laser melting materials, stainless steel and commercially available Al–Si_{10}–Mg alloy materials are used to test materials for electrode printing. The highest H_2-production rate achieved using SC-MEC is 2.89 m^3 d^{-1} at an applied voltage (AV) of 0.9 V and a current density (CD) of 322.1 A m^{-3}. The superior catalytic properties of platinum-coated carbon cloth and Ni alloy-based cathodes allow them to outperform their stainless-steel cathode counterparts in terms of cathodic H_2 recovery values. On the other hand, better gas production is possible with the porous anode (Al-based) because it has a higher surface area-to-volume ratio than the carbon cloth anode.

Open Access Article. Published on 29 1403. Downloaded on 17/02/1405 01:20:45 ..
This article is licensed under a Creative Commons Attribution-NonCommercial 3.0 Unported Licence.

In another study, 3D printed electrodes with different geometries were prepared using a copper-based electrify filament to enhance mass transfer within the cell.[29] According to the study, one of the spiral geometries produced H_2 at a high rate quickly among all other spiral geometries, with a potential and current density of 2 V and 1.5 mA cm^{-2} respectively by using cheese whey wastewater. An additional research piece illustrates the application of Ni Mo-alloyed, 3D printed carbon aerogel cathodes to facilitate the production of extremely conductive using a fused filament 3D printer. The MEC can produce H_2 at a rate of between 0.3 and 0.4 mL min^{-1}.[31] Recently, a novel three-chambered non-3D printed MEC design was fabricated consisting of a membrane-separated common anodic chamber and two cathodic chambers at either end of the anodic chamber.[34] Together, the MFC and MEC produce H_2 to help recover electricity produced by the MFC. The MFC-coupled MEC system's cathodic H_2 recovery is 4.81 mL L^{-1} and 8.89 mL L^{-1} per day. The amount of H_2 that can be produced is directly influenced by the content of organic waste because it contains carbon, hydrogen, and oxygen (C, H, and O).[29] Numerous studies have looked into the possibility of organic wastes producing H_2, with cheese whey wastewater having the highest volume of H_2 production among organic wastes. High concentrations of lactose and lactic acid ($C_{12}H_{22}O_{11}$ and $C_3H_6O_3$) are produced by the use of cheese whey substrate, that yields H_2 of 290 mL g^{-1}. Similarly, of all organic sugars, lactose has the highest H_2 content.[35,36] On the contrary, the material, geometry, physical structures, and active surface area of the electrodes are the main parameters that affect the MEC performance. The most popular types of electrodes used in MEC are ceramic-based, nickel (Ni), platinum (Pt), carbon-based, stainless steel (SS), bio-electrodes (living cell), nickel (Ni), *etc.* can be made by using 3D printing technology.[36–38]

In order to develop a self-sustained, zero-discharge H_2 production system, our research integrates MEC, MFC, ECC, and a PBR. Although the MEC needs an external power source in order to operate effectively. This is resolved by adding an MFC to generate electricity from the same wastewater feedstock, that enhances system sustainability and helps to partially offset the MEC energy needs. However, the MFC uneven voltage output could make it more difficult for stable MEC operation as discussed above. This is avoided by using an ECC, which stabilizes and controls the voltage applied to the MEC while reducing the amount of external energy needed. This guarantees efficient and ongoing H_2 production. Furthermore, one important by-product of MEC-based H_2 generation is CO_2. In a PBR, it is captured and utilized to grow algae instead of being released to atmosphere. This integration ensures zero discharge by reducing reliance on freshwater, recycling treated wastewater for future use. The MFC–ECC–MEC–PBR combination creates a scalable, waste-free, and energy-efficient decentralized H_2 production system that adheres to the principles of the circular economy. Reuse (electricity), regeneration (H_2), and recycling (wastewater) of resources are made possible by energy recovery from waste, that is consistent with the ideas of the circular economy. This strategy encourages resource sustainability, lessens reliance on fossil fuels, and has a minimal negative impact on the environment. Innovative methods for regenerating H_2 from waste guarantee a closed-loop system, improving energy security and supporting a robust and sustainable circular economy. In this review article, scientific discussions have been presented on the following points: (i) the performance of the 3D printed stacked MFC–ECC power the MEC–ECC system; (ii) the performance of series and parallel 3D printed stacked MEC–ECC system; (iii) insights on the development of a prototype stacked MFC–ECC–MEC–PBR (self-sustained and zero discharge) system that delivers H_2 (bioenergy); (iv) strategies to improve the performance of stacked MFC–ECC–MEC–PBR systems using other techniques like use of 3D printed bio-anode. In addition, suggestions and possible future applications of stacked MFC–ECC–MEC–PBR have been presented with the possible future of H_2 energy as a fuel source.

2. Types of MEC system

Fig. 2(a) and (b) represent, SC and dual-chamber (DC) MEC systems are classified according to their configurations. In SC-MEC, both electrodes are positioned in a SC in a SC-MEC, neglecting the need for a membrane.[39–41] However, in DC-MEC, the cathode and anode are divided by a membrane. Anion and cation exchange membrane (AEM and CEM) help obtain pure H_2, prevent microbial H_2 consumption, minimize fuel and bacterial crossover from anode to cathode, and prevent short circuits.[42–44] In addition to reducing bio-contaminations of cathode metal catalysts, the DC arrangement allows control over distinct microbial species in the cathode and anode. On the other hand, high current densities can be achieved because the SC cell minimizes potential loss brought on by the membrane.

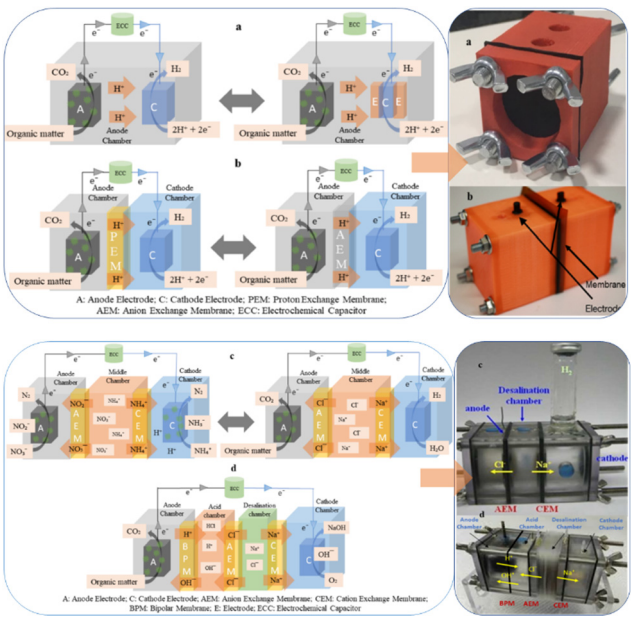

Fig. 2 A schematic and real images of MEC system forms categorized by application and compartment (a) SC-MEC and SC-MEC with sandwich C-electrode[8] (b) DC-MEC with PEM and DC-MEC with AEM[8,45] (c) three-chamber MEC[46] and (d) four chambers MEC.[47,48]

This journal is © The Royal Society of Chemistry 2025

Open Access Article. Published on 29 1403. Downloaded on 17/02/1405 01:20:45 ..
This article is licensed under a Creative Commons Attribution-NonCommercial 3.0 Unported Licence.

2.1 SC-MEC system

In MEC, a variation of MFC, anaerobic bacteria on the anode are utilized to break down organic matter and produce H_2 through the process of electrohydrogenesis.[39] Protons and electrons from the anode are converted to H_2 at the cathode. Since electrohydrogenesis uses less energy and is more environmental friendly than thermochemical or biological methods, it is a promising technology to produce H_2 at a higher yield.[49] Thus, MEC has been extensively studied for improved renewable H_2 production from biomass and wastewater. Recently, the performance of the SC-MEC was assessed at applied voltages ranging from 0.8 to 2.2 V during a six-week operating period.[50] The MEC generated 0.258 m^3 m^{-2} of H_2 over ten cycles at applied voltage of 2.0 V. The MEC demonstrated a constant operating current density of 27.8 A m^{-2} in contrast to the control MEC. An applied voltage increase to 2.2 V results in a decrease in the rate of H_2 production. Another study recovered H_2 using food waste as the substrate, this study combined anaerobic digestion (AD) with SC-MEC treatment using an integrated reactor.[51] The quantity of H_2 produced is 511.02 mL g^{-1} during continuous AD-MEC operation was more than that produced by AD (*i.e.*, 49.39 mL g^{-1}). A different study focuses on a semi-SC-MEC that uses a cellulose dialysis bag to enclose a combined-material anode composed of stainless steel and carbon cloth.[52] The anode was encapsulated to promote the acclimation of bacteria and the formation of biofilms on the anode material. The study of dialysis bags with varying molecular weight cut-offs revealed that the current density was only 12.4 A m^{-2}, and the H_2 production rate at 50 kDa was 0.160 m^3 m^{-2} d^{-1}. In another study, researchers looked at the production of H_2 using a SC-MEC fed with high-strength wastewater and varying electrode materials (metal and carbon), configurations of the reactor.[53] The maximum H_2 production rate of 314 m^3 m^{-3} d^{-1} was recorded in MEC using metal electrodes.

Recently, MEC treatment of combined leachate and dairy wastewater at two days hydraulic retention time (HRT) and an applied voltage of 0.8 V were studied.[54] H_2 can be produced with a power density and a current density of 15 mL L^{-1} d^{-1} and 80 mW cm^{-2} 10 A m^{-2} respectively. In another study source-separated urine could be used to stop H_2 loss in the MEC; the primary cause of the H_2 loss was total ammonium nitrogen from urea hydrolysis.[41] The optimal range for total ammonium nitrogen concentration was 1.17 g N L^{-1} to 1.75 g N L^{-1}. In this range, the rate of H_2 production increased dramatically, from less than 100 L m^{-3} d^{-1} to 520 L m^{-3} d^{-1}. In another study using a nickel electrode, the H_2 production rate in a SC-MEC produced 2.8 mL L d^{-1} and 17.7 mW m^{-2} of power density at pH 7.[55] According to another study, a carbon electrode coated with nano-porous oxide and TiO_2 produced the highest H_2 yield of 0.064 m^3 m^{-3} d^{-1}.[56] In place of more expensive metallic electrodes, carbon electrodes with more-porous coatings may prove to be a viable and cost-effective cathode in the MEC for the production of H_2. A similar study explored that photo-assisted SC-MEC with $ZnFe_2O_4$/g-C_3N_4 cathodes can produce H_2 up to 1.70 m^3 m^{-3} d^{-1}.[57] Another study examined the effects of applied voltages on the performance of the MEC and the anodic biofilm viability during the anaerobic biotransformation of straw waste biomass into green energy.[58] The best H_2 yield was found at 0.8 V after the study investigated applied voltages between 0.5 and 1.0 V, indicating that the highly potential-sensitive mixed electroactive consortia. Another research investigation uses anode modification and biomass enzymatic pre-treatment.[59] In MEC with the coated anode (graphene and iron oxide nanoparticles) at an applied voltage of 0.8 V and moderate mixing, the maximum H_2 production of 224 mL g^{-1} of biomass was achieved. Similar research employs SC-MEC fed with high-strength wastewater to demonstrate electrocatalytic activities and H_2 production.[53] Various electrode configurations, materials (metal and carbon), and electrode distances are used. Using the electrode configuration of stainless steel 304 flat mesh 60 as a cathode and pleated mesh 60 as an anode at a distance of 4 cm from the electrode, the maximum H_2 production rate (HPR) of 314 m^3 m^{-3} d^{-1} with an overall H_2 recovery of 340% was achieved. Another research explored MEC components that were set up in a concentric configuration: a cylindrical graphite felt anode and a platinum-coated titanium mesh cathode. At 0.8 V, the fermentation effluent produced a high H_2 production rate of 6.26 $\pm$ 0.23 L L^{-1} d^{-1}.[60] Another study on H_2 production from glucose was enhanced by adding a specific methane inhibitor (such as chloroform) to inhibit the activity of methanogens in an SC-MEC with a double anode configuration.[61] The maximum H_2 production at 0.8 V is 2.31 and 2.81 m^3 m^{-3} d^{-1} with glucose concentrations of 3 g L^{-1} and 4 g L^{-1}, respectively. The H_2 production increases as the glucose concentration increases. Table 1 shows the overall performance of the SC-MEC system.

The reaction occurs at the anode side:

$$CH_3COO^- + 2H_2O \rightarrow 2CO_2 + 7H^+ + 8e^- \quad (E^\circ = -0.296 \text{ V at pH} = 7) \quad (1)$$

The reaction occurs at the cathode side:

Table 1 Overview of SC-MEC system performance

Type of system	CD (A m^{-2})	AV (V)	CE (%)	H_2 production (m^3 m^{-3} d^{-1})	CHR (%)	Ref.
SC-MEC (dual anode)	286–316	0.8	64–61	2.31–2.81	81–77	61
SC-MEC	27.8	2.0	99.0	1.29	—	50
Semi SC-MEC	15.7	—	—	0.160[a]	—	52
SC-MEC	362.0[b]	0.6	23.0	0.053	81.0	62
SC-MEC	—	0.8	—	6.26[b]	—	60
SC-MEC	—	—	—	1.70	—	57
SC-MEC	—	—	—	314.0	340.0	53
SC-MEC	—	0.8	68.4	6.017[c]	460.4	58
SC-MEC	—	0.8	—	224[d]	—	59
SC-MEC	—	0.8	—	0.06	—	63
AD-MEC	9.87	0.8	—	4.86[b]	—	51
SC-MEC	10	0.8	—	15[e]	—	54
SC-MEC (dual anode)	1355.0[a]	0.8–1.5	—	5.56–10.88	118.0	64

Note: SC-MEC: single chamber MEC [a] Unit of H_2 production/yield and CD: m^3 m^{-2} d^{-1} and A m^{-3} respectively. [b] Unit of H_2 production/yield and CD: L L^{-1} d^{-1} and mA m^{-2} respectively. [c] Unit of H_2 production/yield: mmole of H_2 g^{-1} of COD. [d] H_2 production/yield: mL g^{-1}. [e] H_2 production/yield: mL L^{-1} d^{-1}.

Open Access Article. Published on 29 1403. Downloaded on 17/02/1405 01:20:45 ..
This article is licensed under a Creative Commons Attribution-NonCommercial 3.0 Unported Licence.

$$2H_2O \rightarrow 2e^- + H_2 + 2OH^- \quad (E^\circ = -0.414\ \text{V at pH} = 7) \quad (2)$$

$$E^0_{cell} = E^0_{cathode} - E^0_{anode} = -0.118\ \text{V} \quad (3)$$

2.2 DC-MEC system

Fig. 2(b), DC-MEC system, membranes are used to keep H_2 and oxygen gases apart and from reacting. Membranes have also been used in MEC, most likely to guarantee high H_2 concentrations and prevent bacteria in the anode chamber from utilizing H_2. However, even when a membrane is employed, some researchers have found that the H_2 generated at the cathode is contaminated by other gases (like CO_2) generated at the anode. Additionally, the membrane's presence does not prevent H_2 from diffusing back into the anode chamber. Moreover, methanogenic bacterial degradation and membrane diffusion cause H_2 loss in SC-MEC and DC-MEC, respectively. It is therefore essential to find a barrier to protect the bacterial anode using 3D printed modified AEM or PEM.[45,63]

Recently, a new separator-electrode assembly configuration was created, the cathode was positioned between a hydrophobic polytetrafluoroethylene–(PTFE) membrane and a hydrophilic polyvinylidene difluoride (PVDF) membrane.[65] A low H_2 crossover between the cathode and the anode decreased methanobrevibacter enrichment within anode biofilms in MEC, resulting in an H_2 production rate of 4.53–5.02 $m^3\ m^{-3}\ d^{-1}$ that was significantly higher than that of conventional SC-MEC. Another investigation is the DC-MEC performance with fermentation effluent and AEM or CEM.[66] At 0.8 V applied voltage, the highest yield of H_2 in DC-MEC (1.26 L g^{-1}) by using AEM compared to CEM. In contrast to PEM–MEC, AEM-MECs performed significantly better due to their much higher cathodic H_2 recovery (*i.e.*, a higher proportion of cathodic electrons toward H_2 evolution) and COD removal efficiency (*i.e.*, more electrons to be transferred to the anodes). The observed results may be attributed to the pH imbalance between the anode and cathode sides in PEM-MEC, as opposed to AEM-MEC.[43,67,68] Another study investigated DC-MEC that was operated with a starch-based medium as the anolyte and rice paddy field soil as the anode inoculum.[69] The anode chamber was bio-augmented with Geobacter sulfurreducens strain (YM18) to increase current generation and H_2 production. The highest H_2 production was achieved by using the above stain up to 0.8 L $L^{-1}\ d^{-1}$. Another study used a reduction deposition method to create a hybrid containing ruthenium nanoparticles loaded on conductive carbon nanotubes (Ru/CNTs).[70]

Adopting a cathode electrode coated with Ru/CNTs can produce H_2 at a rate of 0.167 $m^3\ m^{-2}\ d^{-1}$. A different study demonstrates that using MEC in a fuel cell sensor can be an inexpensive online tool for monitoring H_2 production. The H_2 generated in the MEC was oxidized at the fuel cell's anode to produce easily monitored electricity.[71] Table 2 shows the overall performance of the DC-MEC system.

Table 2 Overview of DC-MEC system performance

Type of system	CD ($A\ m^{-3}$)	AV (V)	CE (%)	H_2 production/yield ($m^3\ m^{-3}\ d^{-1}$)	CHR (%)	Ref.
DC-MEC	—	0.8	—	5.31	—	45
DC-MEC (a novel separator)	482.5–515.0	0.8	—	4.53–5.02	90.0	65
DC-MEC	17.13[a]	—	—	0.167[a]	—	70
DC-MEC (AEM)	5.10[a]	0.8	96.0	1.26[c]	85.0	66
DC-MEC	13–14[b]	—	—	0.7–0.8[b]	—	69
DC-MEC	—	0.8	—	10.3[d]	—	42
DC-MEC	0.632[a]	0.8	50.0	0.066[e]	—	72

Note: DC-MEC: double chamber MEC. [a] Unit of H_2 production/yield and CD: $m^3\ m^{-2}\ d^{-1}$ and A m^{-2} respectively. [b] Unit of H_2 production/yield and CD: L $L^{-1}\ d^{-1}$ and mA respectively. [c] Unit of H_2 production/yield and CD: L g^{-1}. [d] Unit of H_2 production/yield and CD: mg H_2 g^{-1} of COD. [e] Unit of H_2 production/yield: L d^{-1}.

2.3 Three-chamber MEC

An alternate, successful, and economical method for achieving simultaneous biogas upgrading, CO_2 recovery, and wastewater treatment is the novel microbial electrolytic capture, separation, and regeneration cell.[7] A bipolar membrane (BPM) and an AEM, respectively, divide the anode chamber, generation chamber, and cathode chamber that make up this system as shown in Fig. 2(c). If an external voltage is applied, electrons from the oxidation of organic matter by bacteria move from the anode to the cathode, where they undergo H_2 evolution and OH accumulation. Water dissociation in the BPM produces H^+ and OH^-, which leads to an acidic regeneration chamber and neutralization of OH^- with H^+ released from substrate oxidation in the anode chamber. In addition to preventing a sharp drop in pH in the anode, BPM has the demonstrated ability to produce acid and alkali in (bio)electrolytic processes more efficiently and economically than traditional AEM and CEM.[73,74] Recently, the alkali solution generated in the cathode first absorbs CO_2 from the biogas input as HCO_3^- and CO_3^{2-}.[7] Owing to the potential differential between the cathode and middle chambers, HCO_3^- and CO_3^{2-} then move *via* AEM to the regeneration chamber, where they recombine with H^+ to generate CO_2. Thus, it is possible to simultaneously achieve biogas upgrading, CO_2 recovery, wastewater treatment, and H_2 production through such a process. In another similar study, the combination of microbial desalination cell (MDC) and MEC has been implemented to improve desalination efficiency and H_2 recovery in three chambers of microbial electrolysis desalination cell (MEDC).[46] The possible reaction that occurs in the three-chamber MEC system is as follows.

Possible reaction at the cathode side:

$$CO_2(aq) + H_2O \rightarrow H^+ + HCO_3^- \quad (4)$$

$$HCO_3^- + OH^- \rightarrow H_2O + CO_3^{2-} \quad (5)$$

Possible reaction at the middle chamber:

$$CO_3^{2-} + H^+ \rightarrow HCO_3^- \quad (6)$$

$$HCO_3^- + H^+ \rightarrow H_2CO_3 \leftrightarrow CO_2(aq) + H_2O \quad (7)$$

2.4 Four-chamber MEC

The microbial electrolysis desalination and chemical production cell (MEDCC) is a novel desalination device for wastewater water treatment that combines the MEC and the MDC.[47] The

 This journal is © The Royal Society of Chemistry 2025

Open Access Article. Published on 29 1403. Downloaded on 17/02/1405 01:20:45 ..
This article is licensed under a Creative Commons Attribution-NonCommercial 3.0 Unported Licence.

water dissociation reaction takes place between the two layers when there is an electric field in the BPM. H^+ migrates through the cation exchange layer and OH^- migrates through the anion exchange layer. We propose a new device using BPM to control pH changes in the anode chamber, eliminate Cl^- and phosphate's detrimental effects, and recover Na^+ in the cell. Fig. 2(d), MEDCC is the name of the apparatus. An anode chamber, an acid-producing chamber, a desalination chamber, and a cathode chamber (the alkali-producing chamber) make up the device's four chambers.[47,48]

3. Additive manufacturing

3D printing, also known as additive manufacturing (AM), has grown rapidly over the last few years. Summarily, 3D printing produces structures in three dimensions by layering materials onto computer-aided design (CAD) models.[25,75,76] This process minimizes human intervention and enables the swift and accurate creation of intricate devices and structures with complicated geometries.[77,78] These encouraging characteristics have led to the application of 3D printing in several industries, including arts, aerospace, medical implants, industrial prototype printing, and aerospace industries. Furthermore, 3D printing has been used in various energy-producing devices, including batteries and solar cells. Recently, 3D printing has been used to fabricate various parts of metal-oxide thermocouples, including reactor bodies, electrodes, and membranes, owing to its growing popularity and applicability.[78–82]

3D printing offers more than fifty different technologies to design and make different materials or objects.[83] ASTM F2792-12a divides these AM technologies into seven process categories: materials extrusion, powder bed fusion, sheet lamination, vat photopolymerization, direct energy deposition, binder jetting, and jetting.[83,84] These technologies can be grouped simply as solid, liquid, and powder-based printers depending on the type of feed material (Fig. 3).[78] FDM involves heating the tip of a non-brittle filament to create a semi-liquid state *i.e.*, subsequently laid down for bonding and cooling. An ultraviolet (UV) lamp or UV laser is used in the stereolithography apparatus (SLA), DLP, continuous liquid interface production (CLIP), and two-photon polymerization (2PP) processes to cure a liquid photopolymer in a vat to solidify it. A part of the 3D printing solution is solidified layer by layer, with each subsequent layer bonded to the preceding layer after a small amount of over-curing.[78,85] Similarly, polyjet technology uses the UV curing principle. The polyjet technique offers higher resolution and can print multiple materials simultaneously except for 2PP. For example, it can print a combination of soft rubber and rigid plastic. Superfine inkjet technology can produce ultrafine droplets with a diameter of less than 1 μm, *i.e.*, 10 times smaller than droplets ejected by traditional inkjet printers. Notably, superfine inkjet technology offers the second-best resolution after the 2PP process.[78] Solid-state sintering involves the use of selective laser sintering (SLS) scans followed by heating powder particles at a temperature close to the melting point so that the powder particles' surfaces soften and fuse.[76,78]

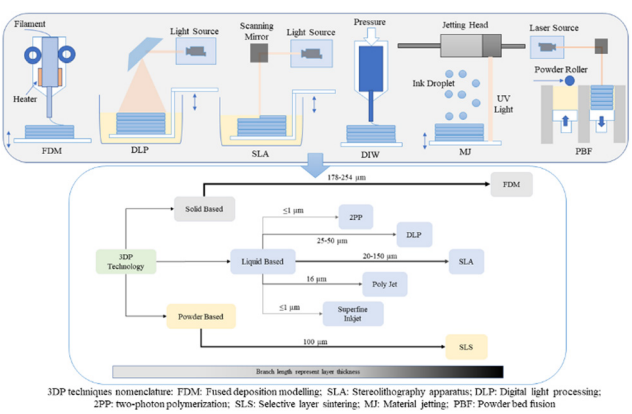

3DP techniques nomenclature: FDM: Fused deposition modelling; SLA: Stereolithography apparatus; DLP: Digital light processing; 2PP: two-photon polymerization; SLS: Selective layer sintering; MJ: Material jetting; PBF: Powder bed fusion

Fig. 3 Classification of 3D printing technologies based on the feed materials utilized.

4. Components for MFC–MEC–ECC–PBR system

4.1 Membranes

AEM or CEM is mostly used in the DC, three and four-chamber MEC system along with BPM (mostly three and four-chamber systems).[48] Two distinct layers make up a BPM: one is anion- and cation-selective. Once applied under reverse potential bias, it exhibits its usual function. In this scenario, the transition region will experience a depletion of electrolyte ions, and solvent dissociation will produce the current carriers. Currently, only two types of solvents have been found to dissociate in BPM: methanol (CH_3OH) and water (H_2O). They are divided into H^+ and CH_3O^- and H^+ and OH^-. When it comes to water splitting, it explains the majority of the uses for BPM processes that have been used till now. In several chemical processes, including the extraction of ions from their corresponding salts, electroextraction, back-extraction, purification of acids and bases, and the synthesis of organic acids and soy protein isolates, BPM has proven to be effective.[47,48,73]

4.2 Electrodes

In MEC, electroactive microbes are important components that impact the performance of H_2 production, apart from the electrodes and other physical components. The anode or cathode biofilms' slow growth kinetics can make complete enrichment difficult, that in turn prolongs the reactor's start-up time. Several studies have used anaerobic sewage sludge as an inoculum source to speed up the enrichment of electroactive biofilms. However, a novel strategy is required to quickly form electroactive biofilms on the electrode surface. Thus, the production of these bio-anodes from 3D printing techniques opens up new possibilities for high-performance MFC–ECC–MEC system.[86]

4.3 Reactor body

In designing MEC, biocompatible materials are favoured because they provide better surfaces on which biofilms can

Open Access Article. Published on 29 1403. Downloaded on 17/02/1405 01:20:45 ..
This article is licensed under a Creative Commons Attribution-NonCommercial 3.0 Unported Licence.

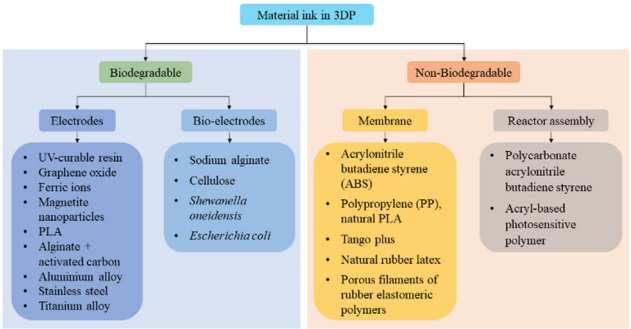

Fig. 4 Schematic of materials use in 3D printing techniques.

adhere and proliferate. MFC reactors were precisely constructed with FDM using biocompatible and nontoxic PLA. Similarly, compared to conventional acrylic fiber material, the quality of the single-chamber MFC reactor made using 3D printing was the same. Furthermore, reactor shapes can be printed again to construct a MEC–ECC system, demonstrating the numerous opportunities that 3D printing has brought about for MEC–ECC design stacking and reactor upscaling.[24,87] The materials used in 3D printing techniques are shown in Fig. 4.

5. Energy storage technology

Various electrical energy storage technologies have been developed over time. Batteries and fuel cells are commonly found in everyday use, while others, such as pumped hydro, flywheels, compressed air, superconducting magnetic systems, and supercapacitors, are geared more toward industrial applications. Among these, batteries are the most extensively used across a wide range of applications, largely due to their exceptional performance.[88,89] Depending on their chemical composition, batteries can be either rechargeable or non-rechargeable. Both types convert chemical energy into electrical energy through redox reactions that occur at the anode and cathode. Rechargeable batteries, however, can reverse this process a limited number of times. Since the 20th century, batteries have become an essential part of modern life, but they are not without limitations.[88–91] Some of the key challenges include: (i) low power density, which restricts their effectiveness in applications that require rapid charge or discharge, (ii) heat generation, which can arise from redox reactions and lead to overheating, thermal runaway, or even fire if not managed properly, and (iii) limited cycle life, as most batteries cannot fully reverse redox reactions during repeated charge and discharge cycles, ultimately reducing their longevity.[88,89,92,93] Due to the challenges mentioned earlier, batteries on their own cannot offer a complete solution for energy storage. An energy storage device that combines durability, safety, and high power or energy capacity would revolutionize the way electric power is generated, distributed, and utilized. Moreover, with growing demands from consumers, industries, and military sectors for more compact and dependable power systems, advancing such technologies remains a key priority in the field of energy storage.[92,94,95]

Electrochemical capacitors (ECCs), supercapacitors, also known as ultracapacitors, offer exceptional power performance, high reversibility, and an impressively long lifespan (exceeding 1 000 000 cycles). Their simple operating mechanism and ease of integration into electronic systems make them highly attractive.[96,97] Additionally, ECCs produce less thermochemical heat due to their straightforward charge storage process. As a result, they are widely used in consumer electronics, memory backup systems, and industrial power and energy management applications. Their presence is also expected to expand into more specialized markets in the near future with increase energy density and low cost. ECCs are classified *via* two primary charge storage mechanisms. The first involves electrostatic charge accumulation at the electrode interface, known as electric double-layer capacitors (EDLCs).[98,99]

The second mechanism, called pseudocapacitance, involves the faradaic process where charges are stored *via* redox reactions on the surface of the electrode. Activated carbon, known for its extensive specific surface area ($\geq$2000 m^2 g^{-1}), is commonly utilized as the active material in these systems. Due to this large surface area, EDLCs have a significantly higher capacity to store energy, often measured in Farads (F). In contrast, traditional dielectric and electrolytic capacitors are measured in much smaller units such as picofarads (pF) and microfarads (μF). Pseudocapacitance occurs at the electrode surfaces where charge storage takes place through faradaic processes. During charging, redox-active materials like RuO_2, Mo_xN, or MnO_2 undergo reduction to lower oxidation states, accompanied by the adsorption or insertion of cations from the electrolyte at or near the electrode surfaces. When the device is discharged, this process is nearly fully reversible. Additionally, printed electronics represent a major advancement in the fabrication of ECCs by offering a range of simple, affordable, and efficient production techniques.[99,100] These methods are versatile, environmental friendly, and allow for the development of cutting-edge ECC designs, including micro, asymmetric, and flexible configurations. This approach enhances the potential of ECCs for use in next-generation electronic devices. Recently, various fabrication techniques for ECCs have been investigated, including electroless plating, thermal evaporation, and electrodeposition. However, these methods can often be intricate and expensive, posing significant challenges for their practical application in commercial settings. 3D printing technology offers a cost-effective, straightforward, and efficient approach that maximizes the capabilities of ECCs. This technique allows for the attainment of desired capacitance at high mass loadings, the creation of complex structures, and the direct fabrication of integrated systems-on-chip. Additional studies on 3D-printed ECCs have explored a variety of materials for their primary electrodes, including activated carbon, graphite, graphene, carbon nanotubes, poly(3,4-ethylenedioxythiophene) polystyrene sulfonate (PEDOT), polyaniline, and MXenes.[14,91,101] In summary, 3D-printed ECCs are a good choice among all electrical energy storage technologies because they offer rapid charging capabilities and enhanced reliability. They have a virtually unlimited lifespan, resist temperature fluctuations, and are non-toxic.

This journal is © The Royal Society of Chemistry 2025

Open Access Article. Published on 29 1403. Downloaded on 17/02/1405 01:20:45 ..
This article is licensed under a Creative Commons Attribution-NonCommercial 3.0 Unported Licence.

6. PBR technology

The benefits of microalgae include their high photosynthetic efficiency, quick growth rate, strong environmental adaptability, and ability to combine with other methods (*e.g.*, wastewater treatment, CO_2 bio-fixation). Microalgae can be grown in a PBR, a specialized device that regulates variables like light, temperature, CO_2, pH, and nutrients.[102,103] The main obstacles to the large-scale planting of microalgae are the design, optimization, and scaling-up of high-efficiency PBR. PBR typically comes in two varieties: open-type and closed-type. The uneven mixing and cell settling in corners are two major problems with using flat panel photobioreactors for algal growth, particularly when bubbling is the only method of mixing biomass.[102,104] Recently, the combination of MFC and PBR systems was used to improve the performance of MFC by utilizing algae as an oxygen source.[20,22,105] In our system, by capturing CO_2 released from the MEC process (from an anode chamber) or other industrial and residential vehicle sources, the combination of MEC technology with a microalgal-based process in MEC-PBR systems could lower GHG from wastewater treatment and H_2 production.

7. Stacked 3D printed MFC–ECC–MEC–PBR system

Researchers predicted that the developments would make it possible to upgrade biogas using CO_2 capture-assisted (PBR) systems in conjunction with MEC.[106] The schematic prediction of a stacked 3D-printed MEC–ECC–PBR system is shown in Fig. 5. The performance of a stacked MEC system also heavily depends on the cathode surface area. Larger surface area cathodes have been shown to increase current density and H_2 production, and the H_2 evolution reaction is frequently the limiting factor in MEC performance. Additionally, the MFC and MEC tests have shown that a reduction in the distance between the electrodes can increase the maximum power output.[8,107,108] Therefore using MEC technology for wastewater treatment, more research is needed to improve the design and develop low-cost electrode materials with a high specific surface area, good conductivity, and high stability. Recently, several anode materials, such as graphite granules, carbon foam, reticulate vitreous carbon, and graphite brush electrodes, have been tested in MEC.[8,44,109]

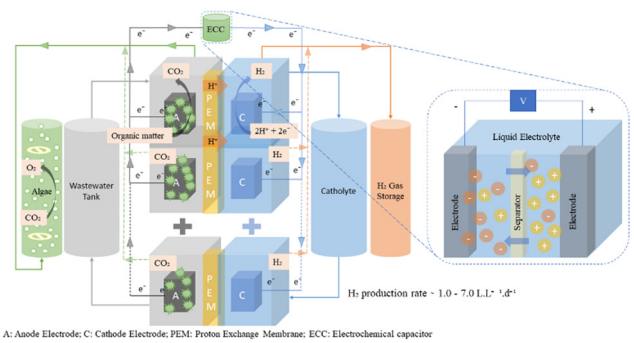

Fig. 5 Schematic of stacked MEC coupled with ECC and PBR.

Table 3 Overall performance of stacked MEC (series or parallel connection)

Type of system	Current (A)	AV (V)	CE (%)	H_2 production (L d^{-1})	CHR (%)	Ref.
S-MEC	1.1	0.1	41.2	0.6	—	110
P-MEC	13.7–16.5[a]	1.36	—	0.71[a]	30–56	111
Sandwich design	—	1.1	66	—	—	113
3DC-MEC	50 to 80[b]	—	99	2.2[b]	—	31
Stacked MEC	49.8[b]	1.0	86.6	258[c]	—	112

[a] Note: unit of H_2 production and CD: L L^{-1} d^{-1} and A m^{-2} respectively. [b] Unit of H_2 Production and current: L CH_4 and mA respectively. [c] Unit of H_2 production: mL d^{-1}; S-MEC and P-MEC: MEC in series and parallel stacked respectively.

A recent study shows that six different MEC cell cassettes, each acting as a single electrolysis cell, were placed in a 120-liter polypropylene tank to make up the MEC reactor setup.[110] The cells were arranged in series inside the wastewater tank. An average of 0.6 L of H_2 per day was produced by a 100 L MEC that was run for a year on raw household wastewater fed at temperatures between 1 °C and 22 °C. Even though it gradually decreased, gas production continued. The applied voltage was gradually increased from 0.6 V to 0.9 V and finally, 1.1 V to acclimate the reactor setup. In another study, electroactive cathodic biofilms were enriched for H_2 evolution reaction in a 10-L single chamber MEC (multi-electrodes system) with a high electrode surface area to volume ratio.[111] The feed was made with lignocellulosic hydrolysate at an organic loading rate of 0.4 g d^{-1} and H_2 production rate of 0.71 L L^{-1} d^{-1}. Based on microbial community analysis, Enterococcus species were identified as the main electroactive bacteria in both the anodic and cathodic groups. Similar work designs the multi-anode and cathode system in the MEC system to produce H_2.[112] The stacked MEC system achieved H_2 flow rate of up to 272 mL d^{-1}. Table 3 shows the overall performance of the stacked MEC system.

8. Applications and future prospect

Recent developments in this technology have led to an increase in the use of 3D printing in MFC–ECC–MEC. Several MFC–ECC–MEC components can be precisely and swiftly fabricated. Interestingly, 3D printing can improve the complex geometrical structures of electrodes with particular properties (like porosity and roughness) to make them more efficient than traditional electrodes. Despite encouraging results, the application of 3D printing for MEC may be limited due to several drawbacks, such as the high cost, low durability, biocompatibility, and electrochemical properties of 3D printed components. Thus, the search for inexpensive yet functional 3D printing materials for MEC components should be continued in future research.[82,114]

8.1 Benefits of MFC–ECC–MEC over solar power systems

The ability of MFC–ECC–MEC to continuously produce capture and utilize bioenergy for the production of H_2 in the absence of

Open Access Article. Published on 29 1403. Downloaded on 17/02/1405 01:20:45 ..
This article is licensed under a Creative Commons Attribution-NonCommercial 3.0 Unported Licence.

solar power is one of its greatest advantages. Sea habitats and polar regions, where sunlight is either rare or non-existent for long periods, can benefit immensely from MFC–ECC–MEC technology. These MFC–ECC–MEC systems use the energy produced by microorganisms' metabolic processes, that continue regardless of light's presence. Therefore, in locations previously limited by solar dependence, MFC–ECC–MEC technology offers a dependable and renewable energy solution, extending the reach of sustainable energy solutions to some of the world's most remote and energy-poor areas. Through the use of photosynthetic organisms, the integration of photobioreactors with MEC presents a novel approach to utilizing CO_2 for algal growth.

8.2 Commercial application for MFC–ECC–MEC–PBR system

There is tremendous potential for increasing the production of H_2 through the combination of 3D printing and biodegradable materials. Through the advancement of technology, 3D printing will enable more affordable mass production and customization of MFC–ECC–MEC–PBR components. Because they produce less long-term waste, biodegradable materials guarantee environmental sustainability. Large-scale uses of this technology have the potential to replace conventional H_2 production methods, that are frequently energy-intensive and dependent on fossil fuels, with ongoing advancements.

8.3 Contribution to the treatment of wastewater

The MFC–ECC–MEC–PBR system provides significant environmental benefits including solutions related to wastewater treatment. Conventional treatment techniques frequently produce large volumes of sludge that adds to environmental pollution and must be disposed of.[115] Conversely, MFC–ECC–MEC–PBR reduces sludge production by using microorganisms to break down organic matter efficiently.[116,117] In addition to raising the water quality, it also reduces the carbon footprint caused by sludge disposal. Therefore, MFC–ECC–MEC–PBR is an important technology for sustainable development because it combines H_2 production with wastewater treatment. Furthermore, by turning waste streams into useful resources, this process improves sustainability in a variety of industries, that is in line with the principles of the circular economy.

8.4 Enhanced manufacturing with 3D printing

The fabrication of a stacked MFC–ECC–MEC system using 3D printing technology is a major and innovative advancement in the technology's affordability and scalability. 3D printing makes it possible to produce MFC–ECC–MEC components precisely, quickly, and with customization, that maximizes the use of available resources and time. This invention lowers production costs and makes it easier to create intricate, highly efficient designs that would be hard or impossible to accomplish using conventional manufacturing methods. The end product is a more widely available and scalable technology that can be used for decentralized energy production, especially in isolated or underserved areas. Additionally, local MFC–ECC–MEC–PBR production promotes resilience and energy independence at the community level.

9. Prediction of future H_2 energy regeneration system

Sustainable H_2 production is essential for decarbonizing industries, lowering reliance on fossil fuels, and promoting clean energy transitions in light of the escalating global energy crisis, freshwater shortage, and climate change concerns. By turning wastewater into H_2 though reducing energy consumption and environmental impact, this research directly addresses these issues. Large-scale deployment in wastewater treatment facilities and renewable energy systems is made possible by the integration of circular economy principles, that encourage resource regeneration, waste minimization, and economic viability. The H_2 fuel cell is a device that converts H_2 energy into electrical energy simultaneously producing heat and water as by-products as per eqn (7) and (8).[118,119] Fig. 6, H_2 cannot be recovered from this system alone; researchers need to combine it with another biological or any other system (*e.g.*, utilizing solar or wind energy) that can do so. If this device or system could be made, it would definitely help to reduce the world's energy, water crisis (use of fossil fuel and pure water for the production of H_2) and carbon impact (GHG). On the other hand, generated H_2 that can be used right away is a suitable solution because H_2 storage and transportation are highly expensive.[120–122]

Moreover, extreme heat waves endanger social and economic activities by raising the demand for electricity and water, that leads to crop losses and forest fires. Due to these gases, solar heat is also retained in the Earth's atmosphere. The basic idea behind the mechanism is that visible light, which is the primary form of solar radiation, travels through the atmosphere and reaches the Earth's surface. Longer-wave infrared radiation is the heat that is released after being absorbed by the land, water, and vegetation. Space would normally be the escape route for this radiation. CO_2, methane (CH_4), nitrous oxide (N_2O), and chlorofluorocarbon (CCl_3F and CCl_2F_2) can absorb some of the infrared radiation that the Earth emits. These pollutants trap heat and can remain in the atmosphere for years or even centuries. This heat no longer radiates into space, this directly leads to the greenhouse effect.[123,124] Nevertheless, any effort to reduce these GHG emissions will undoubtedly support later campaigns to reduce energy consumption. Table 4 tabulate the economic analysis of MEC w.r.t HFC system.

Possible reaction at the anode side:

$$2H_2(\text{Pt catalyst}) \rightarrow 4H^+ + 4e^- \quad (8)$$

Possible reaction at the cathode side:

$$O_2 + 4H^+ + 4e^- \rightarrow 2H_2O \quad (9)$$

Wastewater, agricultural residues, and organic waste are examples of feedstocks that are plentiful and renewable resources for MEC and MFC in a circular economy framework. The availability of essential resources like membranes and 3D printed biodegradable materials affects scalability. In order to

 This journal is © The Royal Society of Chemistry 2025

Open Access Article. Published on 29 1403. Downloaded on 17/02/1405 01:20:45 ..
This article is licensed under a Creative Commons Attribution-NonCommercial 3.0 Unported Licence.

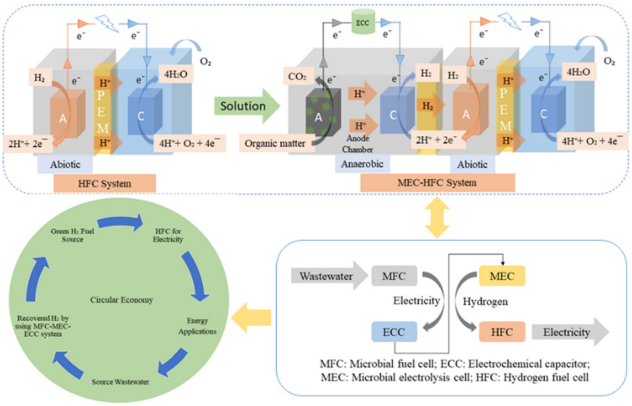

Fig. 6 Schematic representation predictable future of H_2 energy.

lower material costs and increase energy efficiency, MEC need to be further optimized in comparison to traditional H_2 production techniques like gasification, electrolysis and steam methane reforming. Government subsidies, carbon credits, and incentives for H_2 and circular economy projects can also improve affordability. As per Table 4, combining 3D-printed MEC with MFC and ECC offers a scalable and affordable way to produce H_2. This system drastically lowers operating costs by reducing energy input by up to 50–60% (predicted value) when compared to traditional electrolysis. Through removing the need for pricey raw materials and offering an efficient wastewater treatment solution, the use of wastewater as a feedstock further improves economic viability. This system is expected to have a levelized cost of H_2 *i.e.*, 30–40% (predicted value) lower than that of conventional H_2 derived from fossil fuels, making it competitive in the expanding green H_2 market. Through the production of H_2, carbon capture, and resource recovery, this technology not only improves sustainability but also generates economic opportunities by advancing the principles of the circular economy.

10. Conclusion

An increase in global warming and the depletion of natural resources are being caused by the overuse of fossil fuels, including wood, coal, diesel, gasoline, and other petrochemical products. In order to replace the current natural resources, it is crucial to develop environmental friendly and sustainable technology. Additionally, the detrimental effects of wastewater on the environment make treatment necessary. Therefore, the application of 3D printing in MEC has increased as a result of recent developments in the technology. Several MEC components can be fabricated more efficiently using 3D printing, a rapid and accurate fabrication process that has been shown to have promise in the literature. ECC are a simple, efficient, and cost-effective way to extract and utilize energy in the 3D-printed stacked MFC–ECC–MEC–PBR system without the need for additional use of energy. Hence, more research should look into such possibilities for the best possible design and manufacture of 3D printed parts, particularly for stacked MFC–ECC–MEC–PBR systems. Also, by accelerating the process of optimizing custom designs and new materials for the entire system, 3D printing can be a great tool for the commercialization of MFC–ECC–MEC–PBR technology. It is beneficial in markets such as the H_2 energy and desalination sector, with a strong need for precision, customization, flexibility, and complex designs. Customized 3D-printed reactors are crucial to the development of H_2 production because they increase design flexibility, cost effectiveness, and scalability. Their low cost of fabrication, precise structural control, and waste minimization make them ideal for both industrial applications and basic research. For a self-sufficient, zero-discharge system, 3D printing's modular design enables efficient scale-up and integration with MECs, MFCs, and ECCs. Future research should focus on material optimization, durability, and techno-economic viability to speed up commercialization and develop a cost-effective, sustainable H_2 production pathway.

Author contributions

Conceptualization: Mandar S. Bhagat and Chirag Mevada; methodology: Mandar S. Bhagat, Chirag Mevada and Jaini Shah; writing – original draft: Mandar S. Bhagat, Chirag Mevada and Jaini Shah; writing – review and editing: Mandar S. Bhagat, Chirag Mevada, and Matti Mäntysalo; supervision: M. Abdul Rasheed and Matti Mäntysalo; funding acquisition: Matti Mäntysalo.

Data availability

No primary research results, software or code have been included and no new data were generated or analysed as part of this review.

Table 4 Economic analysis of MEC w.r.t HFC system

System	Energy input (kW h kg^{-1} of H_2)	H_2 yield range (L min^{-1})	H_2 flow *versus* output power in HFC		Cost ($ per kg)	Ref.
			(L min^{-1})	(W)		
MEC	1.0–2.2[a]	0.01–3.12[b]	0.1	8–10	4–8	29,33,111,113,125
WE	50–65[c]	1–12[c]	10	800–1000	3–6[d]	126–129
BG	100–111[c]	0.01–0.2[c]	0.2	15–20	2–3[c]	130–133
SMR	3.5–45[c] (depends on feed volume)	5.0–10.0[c]	10	800–1000	0.2–0.7[c]	131,134–136

WE – water electrolysis, BG – biomass gasification, SMR – steam methane reforming. [a] (kW h m^{-3} of H_2). [b] (m^3 m^{-3} d^{-1}). [c] Carbon tax: 52 to 77 $ per tCO_2. [d] 9 kg distilled water: ~1 to 2 $ per kg.

Open Access Article. Published on 29 1403. Downloaded on 17/02/1405 01:20:45 ..
This article is licensed under a Creative Commons Attribution-NonCommercial 3.0 Unported Licence.

Conflicts of interest

There are no conflicts to declare.

Acknowledgements

This study was supported by the Research Council of Finland (grant no. 350309) as part of the CHIST-ERA Transient Electronics for Sustainable ICT in Digital Agriculture (TESLA) Project.

Notes and references

1 B. Hüner, M. Klstl, S. Uysal, İ. N. Uzgören, E. Özdoğan, Y. O. Süzen, N. Demir and M. F. Kaya, *ACS Omega*, 2022, **7**, 40638–40658.
2 K. Fic, A. Platek, J. Piwek and E. Frackowiak, *Mater. Today*, 2018, **21**, 437–454.
3 Y. Koul, V. Devda, S. Varjani, W. Guo, H. H. Ngo, M. J. Taherzadeh, J. S. Chang, J. W. C. Wong, M. Bilal, S. H. Kim, X. T. Bui and R. Parra-Saldívar, *Bioengineered*, 2022, **13**, 8115–8134.
4 K. T. Møller, T. R. Jensen, E. Akiba and H. Wen Li, *Prog. Nat. Sci.: Mater. Int.*, 2017, **27**, 34–40.
5 Y. H. Jia, J. Y. Choi, J. H. Ryu, C. H. Kim, W. K. Lee, H. T. Tran, R. H. Zhang and D. H. Ahn, *Korean J. Chem. Eng.*, 2010, **27**, 1854–1859.
6 Y. Zhang and I. Angelidaki, *Water Res.*, 2014, **56**, 11–25.
7 X. Jin, Y. Zhang, X. Li, N. Zhao and I. Angelidaki, *Environ. Sci. Technol.*, 2017, **51**, 9371–9378.
8 B. E. Logan, *Microbial Fuel Cells*, John Wiley & Sons, Inc., New Jersey, 2007.
9 J. Ditzig, H. Liu and B. E. Logan, *Int. J. Hydrogen Energy*, 2007, **32**, 2296–2304.
10 A. Wang, D. Sun, G. Cao, H. Wang, N. Ren, W. M. Wu and B. E. Logan, *Bioresour. Technol.*, 2011, **102**, 4137–4143.
11 N. Montpart, L. Rago, J. A. Baeza and A. Guisasola, *Water Res.*, 2015, **68**, 601–615.
12 M. S. Bhagat, A. K. Mungray and A. A. Mungray, *J. Indian Chem. Soc.*, 2022, **99**, 100552.
13 M. S. Bhagat, A. K. Mungray and A. A. Mungray, *Water-Energy Nexus*, 2021, **4**, 113–122.
14 C. Mevada, J. Tissari, V. S. Parihar, A. Tewari, J. Keskinen, M. Kellomaki and M. Mantysalo, *J. Mater. Chem. A*, 2024, **12**, 24357–24369.
15 C. Mevada, V. S. Parihar, J. Keskinen, M. Kellomaki and M. Mantysalo, in FLEPS 2024 – IEEE Inter. Conf. on Flex. and Print. Sen. and Sys., Proceed., Institute of Electrical and Electronics Engineers Inc., 2024.
16 M. Sun, G.-P. Sheng, L. Zhang, C.-R. Xia, Z.-X. Mu, X.-W. Liu, H.-L. Wang, H.-Q. Yu, R. Qi, T. Yu and M. Yang, *Environ. Sci. Technol.*, 2008, **42**, 8095–8100.
17 M. C. Hatzell, Y. Kim and B. E. Logan, *J. Power Sources*, 2013, **229**, 198–202.
18 M. C. Hatzell, Y. Kim and B. E. Logan, *J. Power Sources*, 2013, **229**, 198–202.
19 S. Fan, Y. Song, D. Zheng, X. Peng, S. Li, P. Gao and D. Li, *J. Environ. Sci.*, 2025, **152**, 87–98.
20 S. Bolognesi, D. Cecconet, A. Callegari and A. G. Capodaglio, *Environ. Res.*, 2021, **192**, 110263.
21 H. T. Tse, S. Luo, J. Li and Z. He, *Bioprocess Biosyst. Eng.*, 2016, **39**, 1703–1710.
22 H. M. Jiang, S. J. Luo, X. S. Shi, M. Dai and R. B. Guo, *J. Cent. South Univ.*, 2013, **20**, 488–494.
23 A. Hornes, A. Pesce, H. Afonso, A. Morata, M. Torrell and A. Tarancon, *3D Print. Energy Appl.*, 2021, 1–34.
24 Y. Z. Y. Ryan, K. Balachandran, I. Ibrahim, M. Hani Abu Bakar, M. Ismail, W. Lun Ang, E. Hao Yu and S. Su Lim, *Energy Revolution*, 2023, **9**, 1004053.
25 A. Sachdeva and B. Vidyapeeth, *Intagr. Dist. Comput.*, 2020, **13**, 1899–1936.
26 C. Y. Lee, A. C. Taylor, A. Nattestad, S. Beirne and G. G. Wallace, *Joule*, 2019, **3**, 1835–1849.
27 D. Corral, J. T. Feaster, S. Sobhani, J. R. DeOtte, D. U. Lee, A. A. Wong, J. Hamilton, V. A. Beck, A. Sarkar, C. Hahn, T. F. Jaramillo, S. E. Baker and E. B. Duoss, *Energy Environ. Sci.*, 2021, **14**, 3064–3074.
28 K. Kassym and A. Perveen, *Mater. Today: Proc.*, 2020, **26**, 1727–1733.
29 F. Baş and M. F. Kaya, *Fuel*, 2022, **317**, 123560.
30 X. Chen, X. Liu, P. Childs, N. Brandon and B. Wu, *Adv. Mater. Technol.*, 2017, **2**, 1700148.
31 F. Kracke, J. S. Deutzmann, B. S. Jayathilake, S. H. Pang, S. Chandrasekaran, S. E. Baker and A. M. Spormann, *Front. Microbiol.*, 2021, **12**, 696473.
32 Scopus Data (20th Feb, 2025) from **https://www.scopus.com**.
33 V. Kumar, M. Prasad Behera, Y. Lv, B. Pradheepa Kamarajan and S. Singamneni, *Mater. Des.*, 2024, **245**, 113237.
34 D. A. Jadhav, G. Kumar, J. K. Jang and K.-J. Chae, *J. Environ. Manage.*, 2024, **368**, 122209.
35 F. Carvalho, A. R. Prazeres and J. Rivas, *Sci. Total Environ.*, 2013, **445–446**, 385–396.
36 I. K. Kapdan and F. Kargi, *Enzyme Microb. Technol.*, 2006, **38**, 569–582.
37 J. Ren, H. Li, N. Li, Y. Song, J. Chen and L. Zhao, *RSC Adv.*, 2020, **10**, 17163–17170.
38 L. Pötschke, P. Huber, S. Schriever, V. Rizzotto, T. Gries, L. M. Blank and M. A. Rosenbaum, *Front. Energy Res.*, 2019, **7**, 100.
39 D. Call and B. E. Logan, *Environ. Sci. Technol.*, 2008, **42**, 3401–3406.
40 H. Hu, Y. Fan and H. Liu, *Water Res.*, 2008, **42**, 4172–4178.
41 B. Wang, Y. Liu, X. Wang and P. Sun, *Water Res.*, 2023, **247**, 120755.
42 R. A. Chacón-Carrera, A. López-Ortiz, V. Collins-Martínez, M. J. Meléndez-Zaragoza, J. Salinas-Gutiérrez, J. C. Espinoza-Hicks and V. H. Ramos-Sánchez, *Int. J. Hydrogen Energy*, 2019, **44**, 12339–12345.
43 T. H. J. A. Sleutels, H. V. M. Hamelers, R. A. Rozendal and C. J. N. Buisman, *Int. J. Hydrogen Energy*, 2009, **34**, 3612–3620.
44 Y. Zuo, S. Cheng, D. Call and B. E. Logan, *Environ. Sci. Technol.*, 2007, **41**, 3347–3353.
45 S. He, S. Chen, X. Li and Y. Fan, *Chin. J. Environ. Eng.*, 2019, **13**, 1441–1448.
46 M. Mehanna, P. D. Kiely, D. F. Call and B. E. Logan, *Environ. Sci. Technol.*, 2010, **44**, 9578–9583.
47 S. Chen, G. Liu, R. Zhang, B. Qin and Y. Luo, *Environ. Sci. Technol.*, 2012, **46**, 2467–2472.
48 A. Kadier, Y. Simayi, P. Abdeshahian, N. F. Azman, K. Chandrasekhar and M. S. Kalil, *Alexandria Eng. J.*, 2016, **55**, 427–443.
49 N. Wrana, R. Sparling, N. Cicek and D. B. Levin, *J. Cleaner Prod.*, 2010, **18**, S105–S111.
50 W. Cui, Y. Lu, C. Zeng, J. Yao, G. Liu, H. Luo and R. Zhang, *Sci. Total Environ.*, 2021, **780**, 146597.
51 J. Huang, H. Feng, L. Huang, X. Ying, D. Shen, T. Chen, X. Shen, Y. Zhou and Y. Xu, *Waste Manage.*, 2020, **103**, 61–66.
52 S. Rozenfeld, B. Gandu, L. O. Hirsch, I. Dubrovin, A. Schechter and R. Cahan, *Int. J. Energy Res.*, 2021, **45**, 19074–19088.
53 M. Posadas-Hernández, J. L. García-Rojas, S. Khamkure, L. García-Sánchez, T. Gutierrez-Macías, C. Morales-Morales and E. B. Estrada-Arriaga, *Int. J. Hydrogen Energy*, 2023, **48**, 495–513.
54 G. Rani, Z. Nabi, J. Rajesh Banu and K. N. Yogalakshmi, *Renewable Energy*, 2020, **153**, 168–174.
55 C. Mumtha, J. Kabiriyel and P. U. Mahalingam, *Wast. Dispos. Sustain. Energy*, 2023, **5**, 511–524.
56 P. Srivastava, C. González, J. Palma and E. Garcia-Quismondo, *Catal. Today*, 2023, **422**, 114246.
57 S. Song, L. Huang and P. Zhou, *Appl. Microbiol. Biotechnol.*, 2023, **107**, 391–404.
58 F. Ndayisenga, Z. Yu, B. Wang and D. Zhou, *Chem. Eng. J.*, 2023, **469**, 144002.
59 S. Chavan and A. Gaikwad, *Biochem. Eng. J.*, 2023, **193**, 108853.
60 J. Zhang, H. Chang, X. Li, B. Jiang, T. Wei, X. Sun and D. Liang, *Environ. Sci. Pollut. Res.*, 2022, **29**, 89727–89737.
61 J. Zhang, Y. Bai, Y. Fan and H. Hou, *J. Biosci. Bioeng.*, 2016, **122**, 488–493.
62 A. Askari, M. Taherkhani and F. Vahabzadeh, *Korean J. Chem. Eng.*, 2022, **39**, 2148–2155.
63 S. Luo, F. Liu, B. Fu, K. He, H. Yang, X. Zhang, P. Liang and X. Huang, *Water Res.*, 2021, **201**, 117326.
64 D. W. Liang, S. K. Peng, S. F. Lu, Y. Y. Liu, F. Lan and Y. Xiang, *Bioresour. Technol.*, 2011, **102**, 10881–10885.
65 N. Zhao, D. Liang, H. Liu, S. Meng and X. Li, *Chem. – Eng. J.*, 2023, **451**, 138561.

 This journal is © The Royal Society of Chemistry 2025

Open Access Article. Published on 29 1403. Downloaded on 17/02/1405 01:20:45 ..
This article is licensed under a Creative Commons Attribution-NonCommercial 3.0 Unported Licence.

66 Y. Choi, D. Kim, H. Choi, J. Cha, G. Baek and C. Lee, *Bioengineered*, 2023, **14**, 2244759.
67 B. R. Dhar and H. S. Lee, *Environ. Technol.*, 2013, **34**, 1751–1764.
68 G. Zhen, X. Lu, G. Kumar, P. Bakonyi, K. Xu and Y. Zhao, *Prog. Energy Combust. Sci.*, 2017, **63**, 119–145.
69 I. Ochiai, T. Harada, S. Jomori, A. Kouzuma and K. Watanabe, *Bioresour. Technol.*, 2023, **386**, 129508.
70 L. Dai, L. Xiang, M. Zhang, Z. Wen, Q. Xu, K. Chen, Z. Zhao and S. Ci, *ChemElectroChem*, 2022, **9**, e202101584.
71 N. Montpart, M. Baeza, J. A. Baeza and A. Guisasola, *Int. J. Hydrogen Energy*, 2016, **41**, 20465–20472.
72 M. A. M. Asrul, M. F. Atan, H. A. H. Yun, N. A. Wahab, H. H. Hung, J. C. H. Lai and I. A. W. Tan, *ASEAN Eng. J.*, 2024, **14**, 7–17.
73 X. Zhu and B. E. Logan, *Bioresour. Technol.*, 2014, **159**, 24–29.
74 C. Huang and T. Xu, *Environ. Sci. Technol.*, 2006, **40**, 5233–5243.
75 A. Nazir, A. Azhar, U. Nazir, Y. F. Liu, W. S. Qureshi, J. E. Chen and E. Alanazi, *J. Manuf. Syst.*, 2021, **60**, 774–786.
76 T. D. Ngo, A. Kashani, G. Imbalzano, K. T. Q. Nguyen and D. Hui, *Composites, Part B*, 2018, **143**, 172–196.
77 K. C. Obileke, H. Onyeaka, E. L. Meyer and N. Nwokolo, *Electrochem. Commun.*, 2021, **125**, 107003.
78 J. Y. Lee, W. S. Tan, J. An, C. K. Chua, C. Y. Tang, A. G. Fane and T. H. Chong, *J. Membr. Sci.*, 2016, **499**, 480–490.
79 M. P. Browne, F. Novotný, Z. Sofer and M. Pumera, *ACS Appl. Mater. Interfaces*, 2018, **10**, 40294–40301.
80 B. Bian, D. Shi, X. Cai, M. Hu, Q. Guo, C. Zhang, Q. Wang, A. X. Sun and J. Yang, *Nano Energy*, 2018, **44**, 174–180.
81 J. You, R. J. Preen, L. Bull, J. Greenman and I. Ieropoulos, *Sustain. Energy Technol. Assess.*, 2017, **19**, 94–101.
82 T. H. Chung and B. R. Dhar, *Front. Energy Res.*, 2021, **9**, 679061.
83 S. Saleh Alghamdi, S. John, N. Roy Choudhury and N. K. Dutta, *Polymer*, 2021, **13**, 299.
84 A. Zhakeyev, P. Wang, L. Zhang, W. Shu, H. Wang and J. Xuan, *Adv. Sci.*, 2017, **4**, 1700187.
85 S. Scott Crump, *US Pat.*, 5121329, 1992, 1–15.
86 M. C. Freyman, T. Kou, S. Wang and Y. Li, *Nano Res.*, 2020, **13**, 1318–1323.
87 E. Jannelli, P. Di Trolio, F. Flagiello and M. Minutillo, *Energy Proc.*, 2018, **148**, 1135–1142.
88 C. Arbizzani, M. Mastragostino and F. Soavi, *J. Power Sources*, 2001, **100**, 164–170.
89 S. Zhang and N. Pan, *Adv. Energy Mater.*, 2015, **5**, 1401401.
90 C. Santoro, F. Soavi, A. Serov, C. Arbizzani and P. Atanassov, *Biosens. Bioelectron.*, 2016, **78**, 229–235.
91 Z. Han, R. Fang, D. Chu, D. W. Wang and K. Ostrikov, *Nanoscal. Adv.*, 2023, **5**, 4015–4017.
92 M. Arulepp, J. Leis, M. Lätt, F. Miller, K. Rumma, E. Lust and A. F. Burke, *J. Power Sources*, 2006, **162**, 1460–1466.
93 F. Mastragostino Marina and A. C. Soavi, in *Advances in Lithium-Ion Batteries*, ed. B. van Schalkwijk Walter and A. Scrosati, Springer, US, Boston, MA, 2002, pp. 481–505.
94 M. A. Guerrero-Martinez, M. I. Milanes-Montero, F. Barrero-Gonzalez, V. M. Miñambres-Marcos, E. Romero-Cadaval and E. Gonzalez-Romera, *Sensors*, 2017, **17**, 1217.
95 S. Dhanraj Nehate, S. Sundaresh, A. Kumar Saikumar, J. Catanzarite and M. Shao, *J. Electrochem. Soc.*, 1991, **138**, 1539–1548.
96 M. A. Dar, S. R. Majid, M. Satgunam, C. Siva, S. Ansari, P. Arusalan and S. Rafi Ahamed, *Int. J. Hydrogen Energy*, 2024, **70**, 10–28.
97 H. A. Khan, M. Tawalbeh, B. Aljawrneh, W. Abuwatfa, A. Al-Othman, H. Sadeghifar and A. G. Olabi, *Energy*, 2024, **295**, 131043.
98 S. Sahani, H. Mahajan and S. S. Han, *J. Energy Storage*, 2024, **90**, 111808.
99 C. Mevada and M. Mukhopadhyay, in *Handbook of Nanocomposite Supercapacitor Materials IV: Next-Generation Supercapacitors*, ed. K. K. Kar, Springer International Publishing, Cham, 2023, pp. 1–17.
100 C. Mevada and M. Mukhopadhyay, *Ind. Eng. Chem. Res.*, 2021, **60**, 1096–1111.
101 C. Mevada, J. Tissari, V. S. Parihar, A. Tewari, J. Keskinen and M. Mäntysalo, *J. Power Sources*, 2024, **624**, 235529.
102 L. Zhao, G. Zeng, Y. Gu, Z. Tang, G. Wang, T. Tang, Y. Shan and Y. Sun, *Chem. Eng. Sci.*, 2019, **193**, 6–14.
103 N. Castro, J. M. Queirós, D. C. Alves, M. M. M. Fernandes, S. Lanceros-Méndez and P. M. Martins, *Nanomaterials*, 2024, **14**, 525.
104 M. Meagher, J. Tamburro and N. R. Boyle, *Biotechnol. Prog.*, 2024, **40**, e3430.
105 T. Ngoc Dan Cao, T. H. Wang, Y. Peng, H.-Y. Hsu, H. Mukhtar and C.-P. Yu, *Crit. Rev. Biotechnol.*, 2024, **44**, 31–46.
106 T. Gao, H. Zhang, X. Xu and J. Teng, *Water Res.*, 2021, **190**, 116679.
107 M. M. Ghangrekar and V. B. Shinde, *Bioresour. Technol.*, 2007, **98**, 2879–2885.
108 H. Liu, S. Cheng and B. E. Logan, *Environ. Sci. Technol.*, 2005, **39**, 5488–5493.
109 S. K. Chaudhuri and D. R. Lovley, *Nat. Biotechnol.*, 2003, **21**, 1229–1232.
110 E. S. Heidrich, S. R. Edwards, J. Dolfing, S. E. Cotterill and T. P. Curtis, Performance of a pilot scale microbial electrolysis cell fed on domestic wastewater at ambient temperatures for a 12 month period, *Bioresour. Technol.*, 2014, **173**, 87–95.
111 L. Wang, F. Long, D. Liang, X. Xiao and H. Liu, *Bioresour. Technol.*, 2021, **320**, 124314.
112 L. Gil-Carrera, P. Mehta, A. Escapa, A. Morán, V. García, S. R. Guiot and B. Tartakovsky, *Bioresour. Technol.*, 2011, **102**, 9593–9598.
113 H. Guo and Y. Kim, *Biotechnol. Biofuels*, 2019, **12**, 1–23.
114 B. Bian, C. Wang, M. Hu, Z. Yang, X. Cai, D. Shi and J. Yang, *Front. Energy Res.*, 2018, **6**, 50.
115 A. Demirbas, V. Coban, O. Taylan and M. Kabli, *Energy Sources, Part A*, 2017, **39**, 1056–1062.
116 F. Zhang, K. S. Brastad and Z. He, *Environ. Sci. Technol.*, 2011, **45**, 6690–6696.
117 C. M. Werner, B. E. Logan, P. E. Saikaly and G. L. Amy, *J. Membr. Sci.*, 2013, **428**, 116–122.
118 T. Kulkarni and G. Slaughter, *J. Biochips Tissue Chips*, 2015, **5**, 1.
119 D. Choi, I. Jang, T. Lee, Y. S. Kang and S. J. Yoo, *J. Mater. Sci. Technol.*, 2025, **207**, 308–316.
120 T. Galimova, M. Fasihi, D. Bogdanov and C. Breyer, *Appl. Energy*, 2023, **347**, 121369.
121 J. Collis and R. Schomäcker, *Front. Energy Res.*, 2022, **10** 909298.
122 R. Hren, A. Vujanović, Y. Van Fan, J. J. Klemeš, D. Krajnc and L. Čuček, *Renewable Sustainable Energy Rev.*, 2023, **173**, 113113.
123 T. S. Ledley, E. T. Sundquist, S. E. Schwartz, D. K. Hall, J. D. Fellows and T. L. Killeen, *Eos*, 1999, **80**, 453–458.
124 M. Filonchyk, M. P. Peterson, L. Zhang, V. Hurynovich and Y. He, *Sci. Total Environ.*, 2024, **935**, 173359.
125 B. E. Logan, D. Call, S. Cheng, H. V. M. Hamelers, T. H. J. A. Sleutels, A. W. Jeremiasse and R. A. Rozendal, *Environ. Sci. Technol.*, 2008, **42**, 8630–8640.
126 M. M. Rashid, M. K. Al Mesfer, H. Naseem and M. Danish, *Int. J. Eng. Adv. Technol.*, 2015, **4**, 2249–8958.
127 L. Wang, T. Weissbach, R. Reissner, A. Ansar, A. S. Gago, S. Holdcroft and K. A. Friedrich, *ACS Appl. Energy Mater.*, 2019, **2**, 7903–7912.
128 I. Vincent, E. C. Lee and H. M. Kim, *Sci. Rep.*, 2021, **11**, 1–12.
129 F. P. Lohmann-Richters, S. Renz, W. Lehnert, M. Müller and M. Carmo, *J. Electrochem. Soc.*, 2021, **168**, 114501.
130 N. K. Obiora, C. O. Ujah, C. O. Asadu, F. O. Kolawole and B. N. Ekwueme, *Green Technol. Sustainability*, 2024, **2**, 100100.
131 M. Katebah, M. Al-Rawashdeh and P. Linke, *Clean Eng. Technol.*, 2022, **10**, 100552.
132 J. J. Alvarado-Flores, J. V. Alcaraz-Vera, M. L. Ávalos-Rodríguez, E. Guzmán-Mejía, J. G. Rutiaga-Quiñones, L. F. Pintor-Ibarra and S. J. Guevara-Martínez, *Energy*, 2024, **17**, 537.
133 N. K. Obiora, C. O. Ujah, C. O. Asadu, F. O. Kolawole and B. N. Ekwueme, *Green Technol. Sustainability*, 2024, **2**, 100100.
134 X. Sun, G. Nocton and P. W. Roesky, *Chem. Commun.*, 2025, **61**, 1761–1772.
135 A. Magnino, P. Marocco, M. Santarelli and M. Gandiglio, *Adv. Appl. Energy*, 2025, **17**, 100204.
136 A. Di Nardo, M. Portarapillo, D. Russo and A. Di Benedetto, *Int. J. Hydrogen Energy*, 2024, **55**, 1143–1160.